

## Preparation and characterization of nano-crystalline $\text{LiNi}_{0.5}\text{Co}_{0.5}\text{VO}_4$ by tartate precursor combustion method

A. Phuruangrat<sup>1,\*</sup>, T. Thongtem<sup>2</sup>, S. Thongtem<sup>3</sup>

<sup>1</sup>Department of Materials Science and Technology, Faculty of Science, Prince of Songkla University, Hat Yai, Songkhla 90112, Thailand

<sup>2</sup>Department of Chemistry, Faculty of Science, Chiang Mai University, Chiang Mai 50200, Thailand

<sup>3</sup>Department of Physics and Materials Science, Faculty of Science, Chiang Mai University, Chiang Mai 50200, Thailand

Received: 11 October 2010; Accepted: 27 October 2010

---

### Abstract

$\text{LiNi}_{0.5}\text{Co}_{0.5}\text{VO}_4$  has been successfully synthesized by tartate precursor combustion method using  $\text{Li}_2\text{CO}_3$ ,  $\text{Co}(\text{NO}_3)_2 \cdot 6\text{H}_2\text{O}$ ,  $\text{Ni}(\text{NO}_3)_2 \cdot 6\text{H}_2\text{O}$  and  $\text{NH}_4\text{VO}_3$  as a starting materials in deionized water with the subsequent calcination at 450-600 °C for 12 h. The combustion and decomposition of tartate precursor were studied by TGA and compared with tartaric acid. It found weight loss at 50-450 °C. The product showed a inverse spinel  $\text{LiNi}_{0.5}\text{Co}_{0.5}\text{VO}_4$  which confirmed by PXRD. The crystal and particle sizes improved when calcination temperature was increased. Raman and FITR were studied the vibration of product. They detected V-O stretching in  $\text{VO}_4$  tetrahedron, Li-O bending in  $\text{LiO}_6$  octahedron and Li-O-M (M = Ni and Co) stretching. The TEM showed morphologies that composed nano-particle of  $\text{LiNi}_{0.5}\text{Co}_{0.5}\text{VO}_4$ .

**Keywords:** *Lithium ion batteries,  $\text{LiNi}_{0.5}\text{Co}_{0.5}\text{VO}_4$ , Polymerization complex, Cathode material*

---

### 1. Introduction

In recent years, the research on lithium ion secondary batteries has been done to increase the density energy, life cycle and safety of the batteries. One way to increase their density energies is usage of high voltage cathode materials [1-2]. Among of them, the inverse spinel structure transition metal oxides cathode as  $\text{LiNiVO}_4$ ,  $\text{LiNi}_{0.5}\text{Co}_{0.5}\text{VO}_4$  and  $\text{LiCoVO}_4$  can display very well even at a voltage as high as 4.3-4.8 V. Chu et al. [3] reported that the inverse spinel  $\text{LiNi}_{0.5}\text{Co}_{0.5}\text{VO}_4$  has voltage as high as 4.8 V. It is the new candidate cathodes material for Li-ion secondary batteries. Solid state reaction is widely used to prepare cathode materials but it is a

---

\* Corresponding author: Anukorn Phuruangrat  
Chiang Mai University, Chiang Mai 50200,  
Thailand  
Tel +66-53-943-341  
Email [phuruangrat@hotmail.com](mailto:phuruangrat@hotmail.com)

Disadvantage method because of high calcination, bigger particle sizes, impurity and long reaction time [4-5]. Thus, cathode materials were synthesized by solid state reaction due to lower efficiency of electrochemical properties. Therefore, the wet chemical route such as sol-gel [6], polymerization [2], precipitate [7] and hydrothermal [8] is the way to synthesized good physical and chemical properties of cathode material. They are advantage because they have the ability to control homogeneity, particle sizes and economy [4-8]. In this paper present tartate precursor combustion method to synthesized nanopowders  $\text{LiNi}_{0.5}\text{Co}_{0.5}\text{VO}_4$  at low temperature.

## 2. Materials and methods

$\text{LiNi}_{0.5}\text{Co}_{0.5}\text{VO}_4$  was prepared by using  $\text{Li}_2\text{CO}_3$ ,  $\text{Ni}(\text{NO}_3)_2 \cdot 6\text{H}_2\text{O}$ ,  $\text{Co}(\text{NO}_3)_2 \cdot 6\text{H}_2\text{O}$  and  $\text{NH}_4\text{VO}_3$  in molar ratio 0.5:0.5:0.5:1.0 (the molar ratio of Li:Ni:Co:V = 1.0:0.5:0.5:1.0). Each of them were dissolved in deionized water, sequentially mixed them together at room temperature. Then, the solution was adjusted at pH 5 by using  $\text{HNO}_3$ . A saturated tartaric acid solution was slowly added, and heated at  $80^\circ\text{C}$  under magnetic stirring until it became a gelatin (precursor). The precursor was calcined at  $450\text{-}600^\circ\text{C}$  for 12 h. The flow chart in this synthesis was shown in Figure 1.

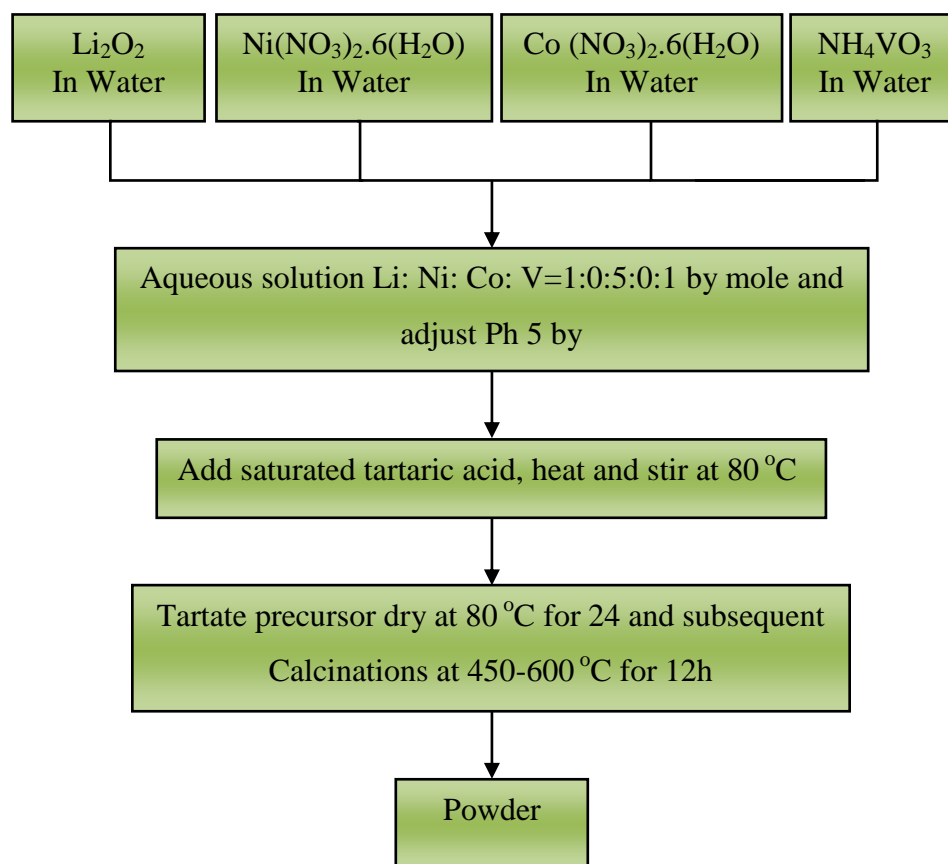


Fig.1. Synthesis process of  $\text{LiNi}_{0.5}\text{Co}_{0.5}\text{VO}_4$

The product was analyzed by TGA-7 Perkin Elmer thermogravimetric analyzer (TGA) with the heating rate of 10 °C/min in a nitrogen atmosphere. The D-500 Siemens powder X-ray diffraction (PXRD) was carried out using Cu K $\alpha$  radiation with the scanning angle range 2 $\theta$  from 10 to 60°, a graphitic monochromatized and a Ni filter. Fourier transform infrared spectroscopy (FTIR) was recorded using by TORNOR 27 OPUS with KBr as diluted agent. Raman spectroscopy (HORIBA JOBIN YVON T64000) was operated using 50 mW Ar Laser with  $\lambda = 514.5$  nm. Transmission Electron Microscopy (JEOL, JEM-2010), Selected Area Electron Diffraction Pattern (SADP) and Energy Dispersive X-ray Spectroscopy (EDX, Oxford instruments INCA) were operated at 200 kV and 15 kV, respectively.

### 3. Results and discussion

Tartate precursor was analyzed using TGA at temperature range 50-600 °C in N<sub>2</sub> atmosphere as shown in Figure 2. Its weight loss is in the temperature rang 50-450 °C. First step, the adsorbed and lattice water in precursor were evaporated at temperature range 50-195 °C. The second step is the decomposition of residual tartaric acid and tartate of lithium, nickel, cobalt and vanadium at 195-290 °C when compared the pure tartaric acid. The third is decomposition and combustion of residual starting materials and other organic compounds at 290-450 °C. After 450 °C, the weight loss of tartate precursor is almost constant. The total weight loss during the thermal analysis is 70 % by weight.

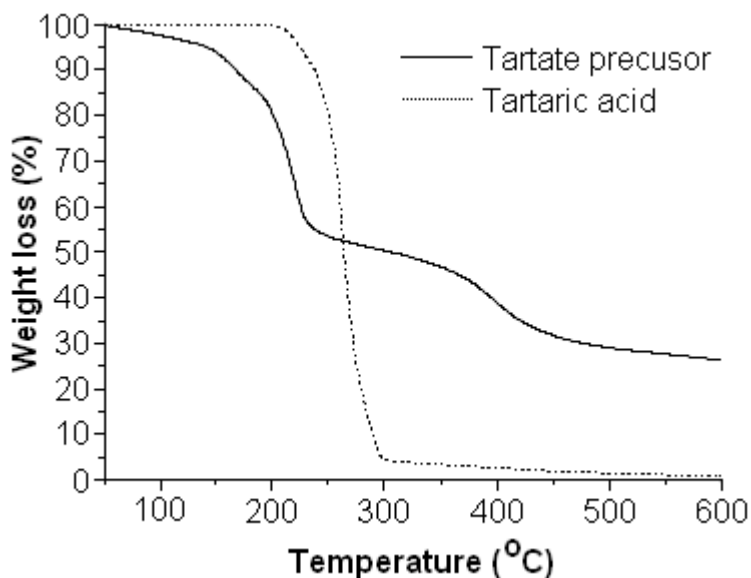


Fig. 2. TGA analysis of nanopowder at temperature range 50-600 °C in N<sub>2</sub> atmosphere

The XRD patterns of LiNi<sub>0.5</sub>Co<sub>0.5</sub>VO<sub>4</sub> at different calcination temperatures are showed in Figure 3 and are identical to the JCPDS standards of LiNiVO<sub>4</sub> (38-1395) and LiCoVO<sub>4</sub> (38-1396) [9]. No impurities such as NiO, CoO, and Co<sub>3</sub>O<sub>4</sub> were detected.

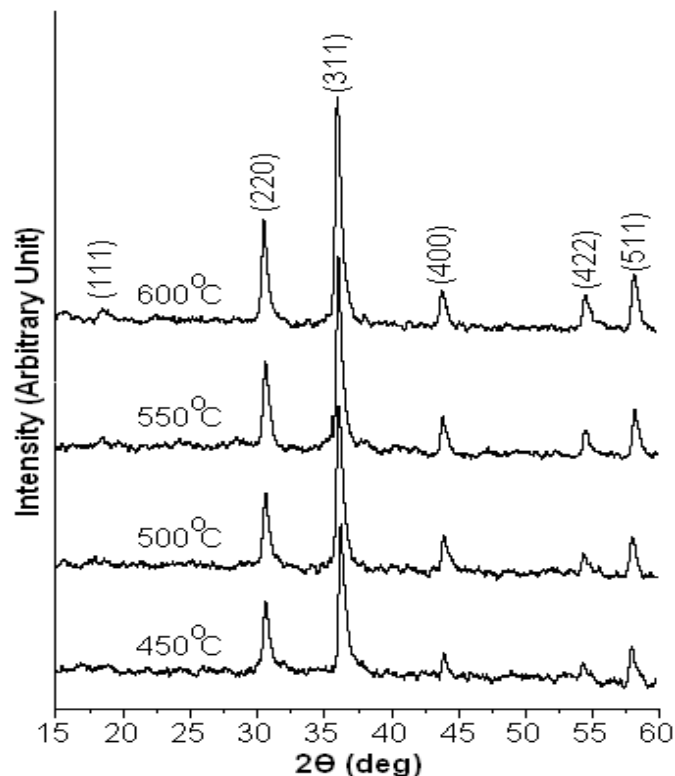


Fig. 3. The XRD patterns of  $\text{LiNi}_{0.5}\text{Co}_{0.5}\text{VO}_4$  at difference calcinations temperatures

The diffraction peaks of product correspond to (111), (220), (311), (400), (422) and (511), respectively. They are dominated the (311) peak at  $2\theta = 36.10$ . The  $2\theta$  position of (311) plane of  $\text{LiNi}_{0.5}\text{Co}_{0.5}\text{VO}_4$  is between the (311) peaks of  $\text{LiNiVO}_4$  and  $\text{LiCoVO}_4$ . The XRD patterns displayed weak (111) and strong (220) peaks. It indicates the predominant inverse spinel structure. That presently, vanadium atoms are in the tetrahedrally coordinated 8a site leading to the higher (220) and lower (111) peaks and the metal ions (Li, Ni and Co atoms) are random in equally octahedron site. At calcination temperature 450–600 °C for 12 h, the spectra become sharper and the intensities are stronger. The degree of crystallinity increases with an increase in the calcination temperature. The degree of crystallinity for inverse spinel structure transition metal oxides cathode was determined from the intensity ratio  $I_{(200)}/I_{(311)} = 0.5$ . It found that the intensities ratio  $I_{(220)}/I_{(311)}$  of  $\text{LiNi}_{0.5}\text{Co}_{0.5}\text{VO}_4$  for calcination temperature at 600 °C for 12 h is 0.48 which showed high crystalline product[2]. The calcination temperature can play the role in improving crystal and grain size of the products. These correspond to the increase in XRD intensities with the increase in the calcinations temperature [1].

The lattice constant ( $a$ ) of  $\text{LiNi}_{0.5}\text{Co}_{0.5}\text{VO}_4$  was calculated from the relation between the plane spacing equation of cubic structure and Bragg's law as shown in Equation 1 [10].

(Eq. 1)

$$a = \frac{\lambda}{2\sin\theta} \sqrt{h^2 + k^2 + l^2}$$

Where,  $\lambda$  is the wavelength of Cu  $K_{\alpha}$ ,  $\theta$  is the Bragg angle and  $hkl$  is Miller indices of lattice plane. At calcination temperature  $600^{\circ}\text{C}$  for 12 h, it is  $8.2436 \text{ \AA}$ . The lattice constant of  $\text{LiNi}_{0.5}\text{Co}_{0.5}\text{VO}_4$  is between those of  $\text{LiNiVO}_4$  and  $\text{LiCoVO}_4$ . It could be seen that nearly the cell constant of  $\text{LiNi}_{0.5}\text{Co}_{0.5}\text{VO}_4$  ( $a = 8.2492 \text{ \AA}$ ) when calculated from lattice constants of  $\text{LiNiVO}_4$  and  $\text{LiCoVO}_4$  [11].

For inverse spinel structure transition metal oxides as  $\text{LiNiVO}_4$ ,  $\text{LiNi}_{0.5}\text{Co}_{0.5}\text{VO}_4$  and  $\text{LiCoVO}_4$  have  $F_{d3m}$  ( $O_h^7$ ) symmetry of which five modes are Raman active ( $A_{1g} + E_g + 3F_{2g}$ ) and four modes are inferred active ( $4F_{1u}$ ) [12]. Raman spectra (Figure 4) was observed in the  $700\text{-}850 \text{ cm}^{-1}$  can be attributed to the stretching vibration of  $\text{VO}_4$  tetrahedron.  $\text{LiNi}_{0.5}\text{Co}_{0.5}\text{VO}_4$  has strong frequency band at  $801.16 \text{ cm}^{-1}$  corresponds to the stretching mode of  $\text{VO}_4$  tetrahedron with an  $A_{1g}$  symmetry, whereas the band stretching at  $314.90 \text{ cm}^{-1}$  corresponds to the bending mode of  $\text{VO}_4$  tetrahedron with an  $E_g$  symmetry. The two stretching frequencies band at  $256.23$  and  $411.81 \text{ cm}^{-1}$  are the vibration of  $\text{LiO}_6$  octahedron. The stretching vibration of  $\text{Li-O-M}$  ( $M = \text{Ni}$  and  $\text{Co}$ ) was detected at  $470.22 \text{ cm}^{-1}$ .

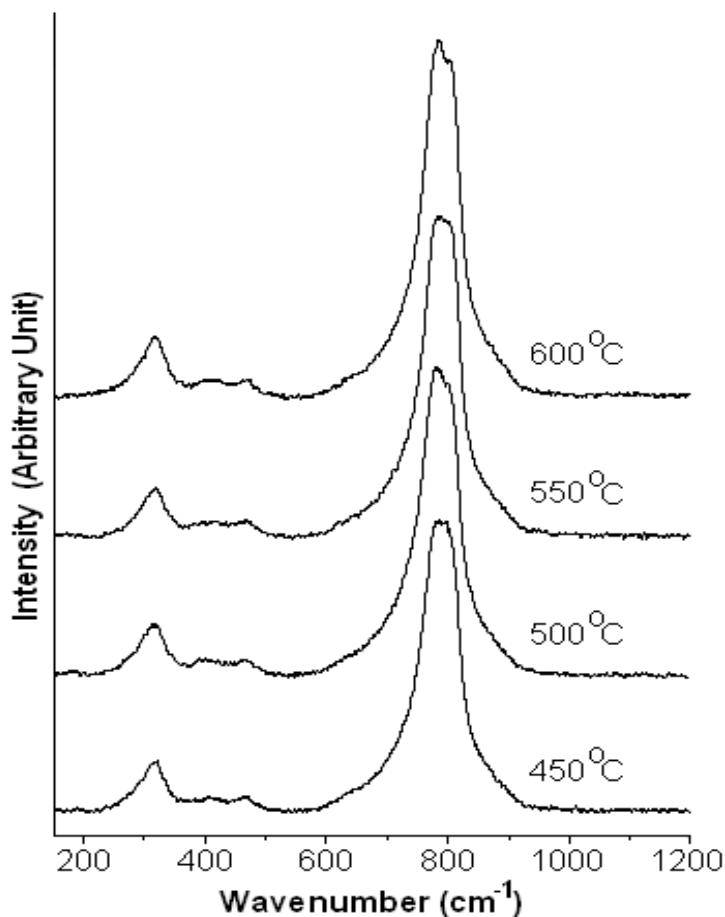


Fig.4. Raman spectra of nanopowder

FTIR spectra of  $\text{LiNi}_{0.5}\text{Co}_{0.5}\text{VO}_4$  is showed in Figure 5. The asymmetric stretching vibration of  $\text{VO}_4$  tetrahedron was showed the broad band at  $810\text{-}850 \text{ cm}^{-1}$  and weak band around  $900 \text{ cm}^{-1}$  assigned to be the symmetric stretching mode in the symmetric stretching mode of  $\text{VO}_4$  tetrahedrons.

In addition, oxygen atom in the  $\text{VO}_4$  tetrahedron can form bond with Li and Co or Ni atom which can lead to some asymmetry. Hence the broad band around  $810\text{--}850\text{ cm}^{-1}$  are tentatively assigned to be the asymmetrical stretching mode in the distorted  $\text{VO}_4$  unit [2, 6]. If it can be considered that all Li atoms are accommodated in octahedron  $\text{LiO}_6$  environments, then Raman- and IR-active modes are normally split into  $(A+2B)$ .  $\text{LiO}_6$  octahedrons have vibrations in IR modes observed at  $410\text{ cm}^{-1}$  corresponding to  $\nu(\text{Li-O})$  [1,4].

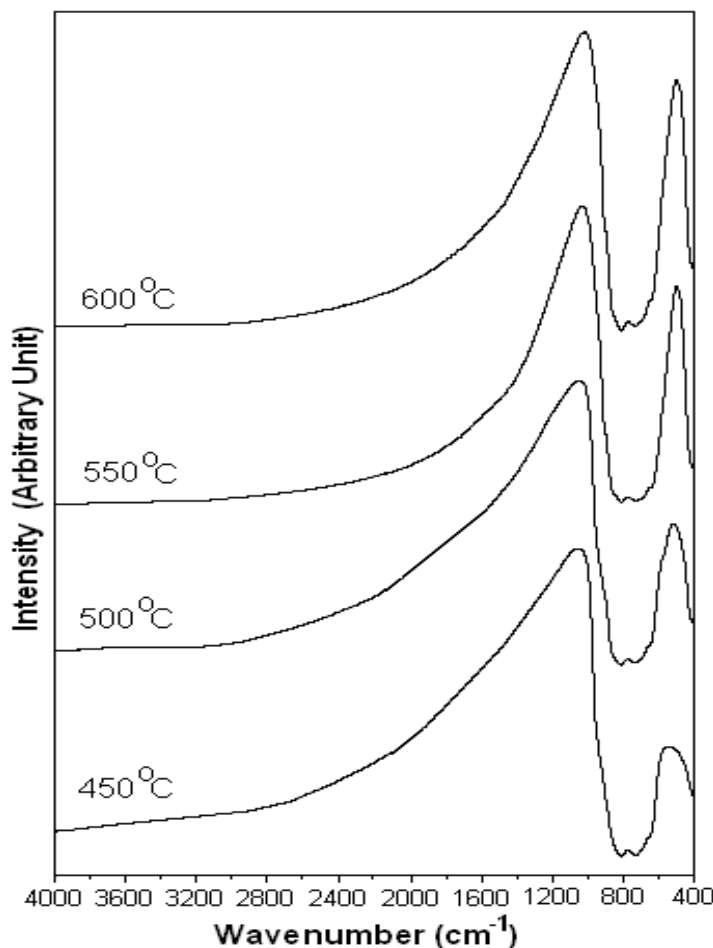


Fig. 5. FTIR spectra of  $\text{LiNi}_{0.5}\text{Co}_{0.5}\text{VO}_4$

TEM images and SAED patterns of  $\text{LiNi}_{0.5}\text{Co}_{0.5}\text{VO}_4$  with 450–600 °C calcination temperature for 12 h are shown in Figure 6. At 450 °C for 12 h, the grain size is 20–80 nm. When increased calcination temperature to 600 °C, the grain size is 200–700 nm due to the effect of calcination temperature which corresponded the XRD patterns. Their SAED patterns show a ring patterns which indicated that polycrystalline  $\text{LiNi}_{0.5}\text{Co}_{0.5}\text{VO}_4$ . The diffraction planes are (111), (220), (311), (400), (422), (511) and (533), respectively.

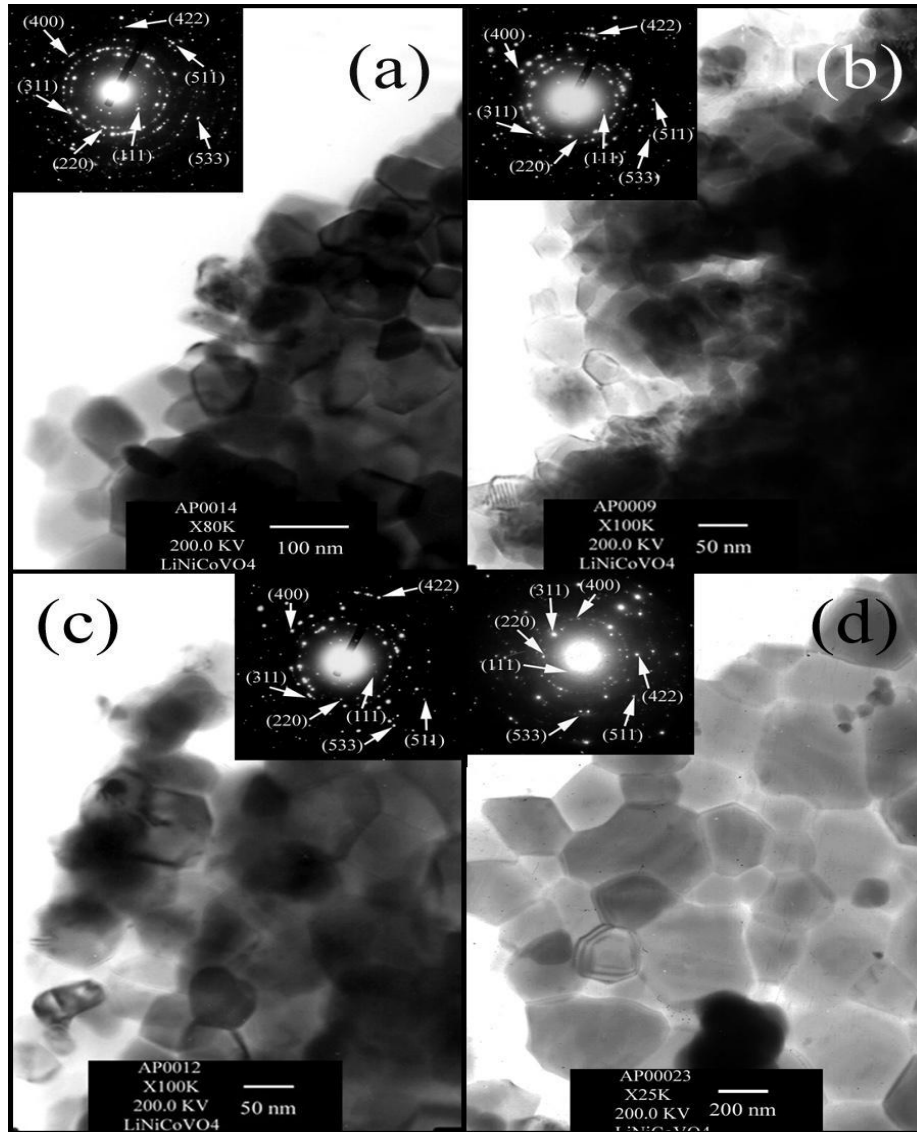


Fig. 6. TEM images and SAED patterns of  $\text{LiNi}_{0.5}\text{Co}_{0.5}\text{VO}_4$  with 450-600 °C calcination temperature for 12 h

#### 4. Conclusion

$\text{LiNi}_{0.5}\text{Co}_{0.5}\text{VO}_4$  was synthesized by tartate precursor combustion method. TGA show the weight loss tartate precursor at 50-450 °C in  $\text{N}_2$  atmosphere. The phase and morphologies were studied by XRD, SAED and TEM. XRD pattern and TEM images show that the  $\text{LiNi}_{0.5}\text{Co}_{0.5}\text{VO}_4$  started to form at 450 °C and its particle sizes is 20-80 nm which has relatively larger specific surface and more favorable for lithium-ion migration as the cathode materials. When increase temperature calcination, it lead to improve the crystalline and grain size of products.

## Acknowledgements

We are grateful to the Thailand Research Fund, Bangkok for financially supporting the research, Graduate School of Chiang Mai University for general funding.

## References

- [1] Liu , J.R., Wang , M., Lin , X., Yin , D.C., Huang , W.D. (2002) . Citric acid complex method of preparing inverse spinel  $\text{LiNiVO}_4$  cathode material for lithium batteries. *J. Power Source* , 108 ,113-116.
- [2] Phuruangrat , A., Thongtem , T., Thongtem , S. (2007) . Preparation and characterization of nano-crystalline  $\text{LiCoVO}_4$  and  $\text{LiNiVO}_4$  used as cathodes for lithium ion batteries. *J. Ceram. Process. Res*, 8 ,450-452.
- [3] Chu , P.P., Huang , D.L., Fey , G.T.K. (2000) . Solid-state  $^7\text{Li}$  NMR studies of inverse spinel  $\text{LiNi}_x\text{Co}_{1-x}\text{VO}_4$  cathode materials. *J. Power Source*, 90 , 95-102.
- [4] Vivekanandhan , S., Venkateswarlu , M., Satyanarayana , N. (2004) . Glycerol-assisted gel combustion synthesis of nano-crystalline  $\text{LiNiVO}_4$  powders for secondary lithium batteries. *Mater. Lett*, 58 ,1218-1222.
- [5] Chen , W., Mai , L.Q., Xu , Q., Zhu , Q.Y., Yang , H.P. (2003) . Novel soft solution synthesis and characterization of submicromic  $\text{LiCoVO}_4$ . *Mat. Sci. Eng. B*, 100, 221-224.
- [6] Mai , L.Q., Chen , W., Xu , Q., Zhu , Q.Y., Han , C.H., Guo , W.L. (2003), Influence of surface modification on structure and electrochemical performance of  $\text{LiNi}_{0.5}\text{Co}_{0.5}\text{VO}_4$ . *Solid State Ionics*, 161, 205-208.
- [7] Fey , G.T.K., Chen , K.S.(1999).Synthesis, characterization, and cell performance of  $\text{LiNiVO}_4$  cathode materials prepared by a new solution precipitation method. *J. Power Source*, 81-82 ,467-471.
- [8] Thongtem , T., Phuruangrat , A., Thongtem , S. (2006) . Analyses of nano-crystalline  $\text{LiCoVO}_4$  prepared by solvothermal reaction. *Mater. Lett* , 60 , 3776-3781.
- [9] Powder Diffract. File, JCPDS Internat. Centre for Diffract Data, U.S.A., (2001).
- [10] Suryanarayana , C., Norton , M.G. X-ray Diffraction A Practical Approach, *Plenum Press*, New York .(1998). 97-236.
- [11] Liu , Y., Xu , Y., Li , J.P., Zhang , B., Wu , D., Sun , Y.H. (2006) . Synthesis of  $\text{CdS}_x\text{Se}_{1-x}$  nanorods via a solvothermal route. *Mater. Res. Bull* , 41 , 99-109.
- [12] Fey , G.T.K., Huang , L.D. (1999) . Synthesis, characterization and cell performance of inverse spinel electrode materials for lithium secondary batteries. *Electrochim. Acta* , 45 ,295-314.